Towards high-performance long-pulse operation with combined LHCD and ECCD in WEST

T. Fonghetti, P. Manas, R. Dumont, J-F. Artaud, C. Bourdelle, F.J. Casson[1], J. Cazabonne, R. Coelho[2], N. Cummings[1], L. Delpech, P. Maget, J. Morales, Y. Savoye-Peysson, M. Schneider[3], E. Vergnaud and the WEST team[4]

CEA, IRFM, F-13108 Saint-Paul-lez-Durance, France

[1]CCFE, Culham Science Centre, Abingdon, OX14 3DB, UK

[2]Instituto de Plasmas e Fusao Nuclear, Instituto Superior Técnico, Universidade de Lisboa, 1049-001, Lisboa, Portugal

[3]ITER Organization, Route de Vinon-sur-Verdon, 13067 St. Paul-lez-Durance Cedex, France

[4]see http://west.cea.fr/WESTteam

Introduction

Achieving long-pulse operation [1] is a key milestone in preparing for steady-state scenarios in next-generation tokamaks like ITER, and in addressing the ageing of plasma-facing components such as the divertor, which is heavily exposed. WEST, a tungsten (W) environment tokamak, is specifically designed for such long-duration discharges, notably thanks to its strong non-inductive current drive capability, with up to 7 MW of Lower Hybrid Current Drive (LHCD) [2]. In 2025, a new record was set on WEST with a plasma duration of 1337 seconds and an injected energy of 2.61 GJ, guided by integrated modelling [3]. The simulations were carried out using the High-Fidelity Plasma Simulator (HFPS), an IMAS-compatible version of the integrated modeling suite of codes JINTRAC [4], widely used across European machines. This modelling workflow enables the self-consistent predictions of the 1D plasma profiles (electron density n_e, electron and ion temperature T_e, T_i, and plasma current density j) through the JETTO transport solver, together with physics-based models, extensively described in [3]. In particular, it features full-radius turbulent heat and particle transport using TGLF-sat2 [5], as well as current drive and heating sources computed via the Heating and Current Drive (H&CD) workflow [6]. The EC source is predicted with the widely validated beam-tracing code TORBEAM [7] and the LHCD source is predicted with the heuristic model extracted from METIS [8,9], together with a scaling law for the CD efficiency [10], fitted from Tore Supra and JET experiments and validated on WEST [3]. Yet, the absence of distribution function consistent evolution prevents synergetic effects to be captured. A notable addition to the framework is the self-consistent prediction of sawtooth crashes, using the Porcelli model [11] for the mode triggering and the Kadomtsev model [12] to describe magnetic reconnections. This is needed in scenarios with large on-axis current-drive. Using this integrated toolset, the

operational domain — spanning LHCD power, plasma current, and electron density — was optimized and post-prediction experiments confirmed the predictions [3]. Building on these results, the study is extended to explore Electron Cyclotron (EC) waves, in both heating (ECRH) and current drive (ECCD) configurations. The objective is to find the optimal trade-off between MHD stability and enhanced performance in terms of plasma energy content and confinement, within the framework of long-pulse scenarios on WEST.

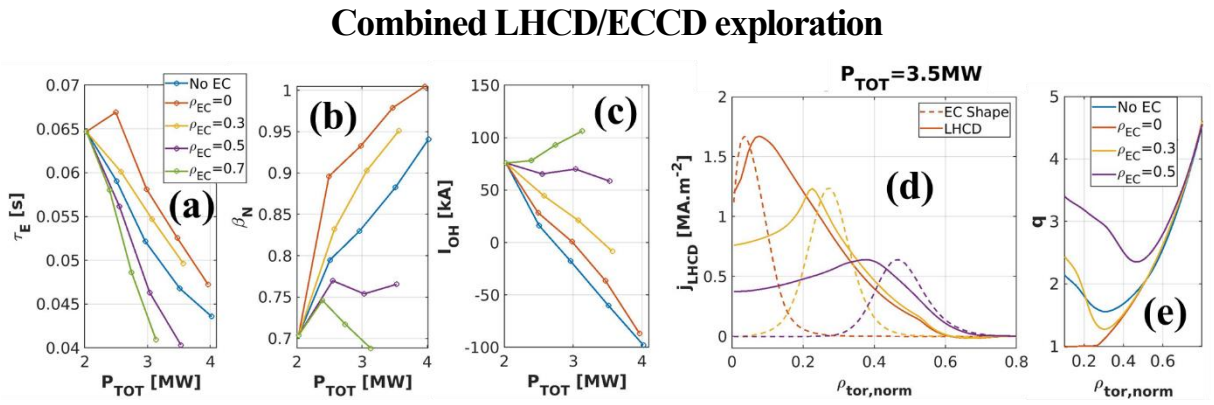

Fig 1. Energy confinement time **(a)**, normalized beta **(b)** and ohmic current **(c)** as a function of the total heating power for different heating schemes: LHCD-only in blue and several ECCD/LHCD combinations with different EC deposition locations in other colors. Corresponding LHCD/ECCD current deposition shape **(d)** and safety factor profile **(e)** for three explored cases keeping the same colors as (a-c) and at total power of 3.5 MW.

ECCD provides localized heat and current-drive sources thanks to flexible steering mirrors at the launcher [13]. In this study, the toroidal injection angle was set to get the largest CD, while the poloidal angle was scanned to get different deposition locations from on-axis (ρ_{EC}=0) to far off-axis (ρ_{EC}=0.7). Also, different EC power amplitude are applied on top of an LHCD-only discharge at I_P=300 kA, P_{LHCD}=2 MW and n_{el}=3.10^{19}m^{-3} to identify the best trade-off between improved stability and performances. The results can be observed in Figure 1. In particular, the stored energy increases as the deposition is shifted towards the axis (Figure 1a-b), as it was previously observed in EAST [14], leading to an increase of the energy confinement time and the normalized beta. This can be explained by larger net heat fluxes crossing all magnetic flux surfaces when the energy is deposited centrally in the plasma, enabling larger equilibrium electron temperature gradients if turbulent transport remains similar. At the same time, the LHCD efficiency increases with the energy confinement time and the ECCD efficiency increases with the electron temperature — monotonously increasing towards the core — at the wave absorption location. For instance, the inductive current is also minimized with central ECCD and eventually reaches similar values as the LHCD-only case (Figure 1c), despite a smaller ECCD efficiency, compared to LHCD. Another point of note is that LHCD current profile was observed to be steered by ECCD (Figure 1d), also reported on EAST [15]. This is

observed when a sufficiently large amount of EC power is applied on top of LHCD, and is shown to have a large effect on the safety factor (q) profile (Figure 1e), which has direct implications in terms of turbulence and stability.

The effect of adding central ECRH

As mentioned previously, the q profile has strong implications on the turbulent transport. For instance, performing stand-alone TGLF scans in magnetic shear and normalized electron temperature gradient (Figure 2a) enables to identify a reduction of turbulence at negative shear in which larger electron temperature gradients can be reached at fixed turbulent heat fluxes. Transport stiffness and critical gradients for the different cases are compared in Figure 2b. In particular, the off-axis ECCD (ρ_{EC}=0.3) case presents large critical gradient and low stiffness, prone to reaching large gradients at a reduced cost in terms of turbulence, referred to as Internal Transport Barrier (ITB). This is performed by adding a gradually increasing central ECRH source up to 2 MW in the HFPS simulations. The result is added on top of stand-alone TGLF simulations with full squares. On the other hand, central and far off-axis ECCD (ρ_{EC}=0.5) temperature gradients are limited by very stiff transport, low critical gradient and, for central ECCD only, by sawteeth events. This is confirmed from the energy confinement time and normalized beta (Figure 2c-d) where off-axis ECCD cases feature larger performances compared to central ECCD.

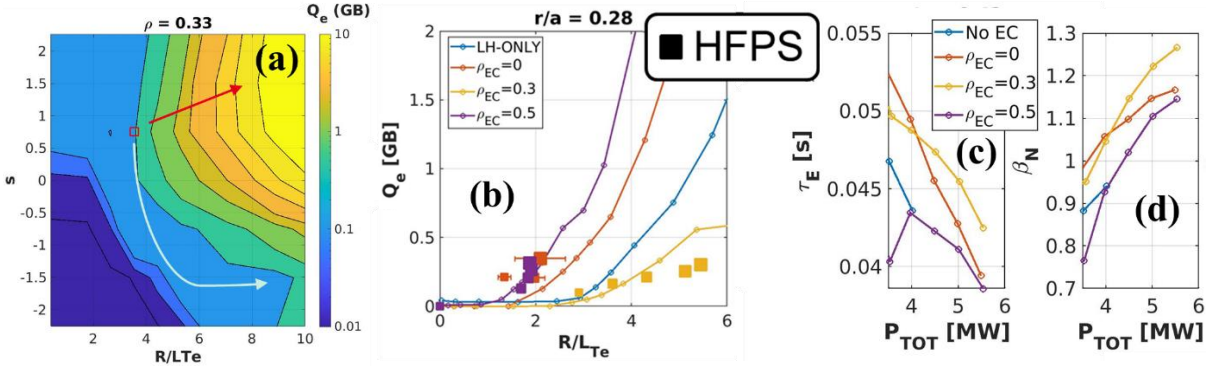

Fig 2. (a) TGLF stand-alone 2D (magnetic shear s – normalized electron temperature gradient R/LTe) scan for a given reference LHCD-only simulation at 3.5 MW. **(b)** TGLF stand-alone R/LTe scans for 4 cases at 3.5 MW featuring different plasma heating schemes and different plasma conditions (full line). HFPS simulations with gradually increasing central ECRH power up to 2 MW are added on top (squares). Radial location corresponds to the q profile reversal of the off-axis ECCD case (orange). Energy confinement time **(c)** and normalized beta **(d)** evolution when adding central ECRH on top of previous HFPS simulations with 3.5 MW of total power.

Linear MHD stability with ECCD

Previous conclusions hold only if the ITB scenario remains MHD stable. Experimental observations from Tore Supra and WEST have shown that the reversed q-profiles are particularly prone to MHD instabilities, most notably Double Tearing Modes (DTM) [16]. In

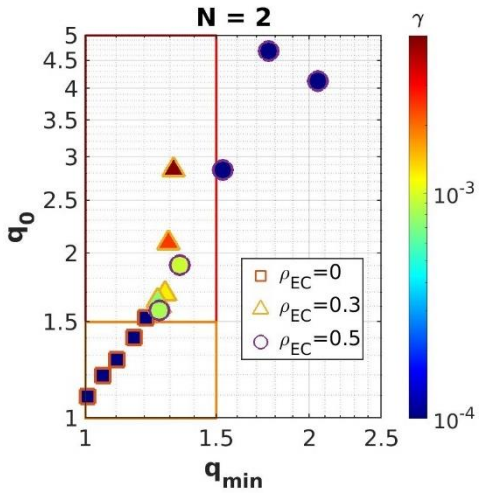

Figure 3. Growth rate of the N=2 modes as a function of q0 and qmin, for three different HFPS simulations turning off ECCD, computed using resistive MHD with MARS [18]

these unstable plasmas, both confinement and CD efficiency are degraded [17], which can ultimately lead to a disruption. This sensitivity is illustrated in Figure 3, which presents resistive MHD simulations of n=2 modes. Although these simulations do not include diamagnetic stabilization effects — leading to a conservative (pessimistic) estimate of the stability — they still highlight the fragility of the scenario. For example, the ECCD case that gives the best performance is also the most unstable to n=2 modes, due to a DTM located around q=3/2. In contrast, the more off-axis case could give access to MHD stable $q_{min} > 2$ operation. In the domain with DTM on q=2 (n=1 modes), the situation is also not ideal. In both cases, diamagnetic rotation may provide linear stabilization of the modes, but the scenario remains experimentally fragile.

Conclusion

The addition of a central ECCD source on top of LHCD was identified to be an improvement over the current LHCD-only WEST long pulses. In particular, these new scenarios are more MHD stable without q profile reversal, have larger performances while providing similar non-inductive current, enabling low loop voltage plasma operation. On the other hand, an off-axis CD source can highly modify turbulent transport characteristics. The addition of a central ECRH source potentially triggers ITB accompanied by larger performances but MHD stability becomes more problematic. These scenarios require a careful monitoring of the q profile by increasing q_{min} above 2 or decreasing the q reversal. This will be explored in the WEST upcoming experimental campaigns with the new 3 MW EC system.

References

[1] X. Litaudon, et al., Nucl. Fusion, 64, 015001 (2024).
[2] J. Bucalossi, et al. Nucl. Fusion, 62, 042007 (2022).
[3] T. Fonghetti, et al., Nucl. Fusion, 65, 056018 (2025).
[4] M. Romanelli, et al., Plasma and Fusion Research, 9, 3403023 (2014).
[5] C. Angioni, et al., Nucl. Fusion, 63, 126035 (2022).
[6] M. Schneider, et al., Nucl. Fusion, 61, 126058 (2021).
[7] E. Poli, et al., Comp. Phys. Communications, 225, 36-46 (2018).
[8] R. Dumont, et al., Phys. Plasmas, 7, 4972–4982 (2000).
[9] J.-F. Artaud, et al., Nucl. Fusion, 58, 105001 (2018).
[10] M. Goniche, et al., AIP, 787, 307–310 (2005).
[11] F. Porcelli, et al., Plasma Phys. Control. Fusion, 38, 2163 (1996).
[12] B. B. Kadomtsev, et al., Soviet Journal of Plasma Phys., 1, 389-391 (1975).
[13] T. Fonghetti, et al., EPJ Web of Conferences, 277, 02006 (2023).
[14] M. Li, et al., Nucl. Fusion, 63, 046019 (2023).
[15] W. Choi, et al., Annual Meeting of the APS Division of Plsma Phys., Oral contribution (2024).
[16] P. Maget, Nucl. Fusion, 45, 69-80 (2005).
[17] Y. Peysson and Tore Supra Team, Nucl. Fusion, 41, 1703 (2001).
[18] P. Maget, et al., Plasma Phys. Control. Fusion, 67, 045005 (2025).